

Dehydrogenation of 1,4-cyclohexadiene on Si(001): A first-principles study

Jae-Kwon Ko and Jun-Hyung Cho*

BK21 Program Division of Advanced Research and Education in Physics, Hanyang University, 17 Haengdang-Dong, Seongdong-Ku, Seoul 133-791, Korea

(Received 16 November 2007; revised manuscript received 19 February 2008; published 18 March 2008)

The adsorption and reaction of 1,4-cyclohexadiene on the Si(001) surface are investigated by first-principles density-functional calculations. We find that there are two kinds of single di- σ bonding configurations: One is the on-top (OT) structure on top of a single Si dimer and the other is the end-bridge (EB) structure across the ends of two adjacent Si dimers in the same dimer row. Formation of the OT and EB structures is kinetically facilitated through the π -complex precursor state in which the electron-deficient down Si atom of the buckled dimer attracts the π bond of 1,4-cyclohexadiene. However, there exists a drastic difference in dehydrogenation kinetics of the two single di- σ bonding configurations. Dehydrogenation of the OT structure hardly takes place because of the existence of a high activation barrier of 1.34 eV, whereas that of the EB structure is kinetically feasible at room temperature with a relatively lower activation barrier of 0.68 eV. Thus, we can say that the recently observed dehydrogenation process in the single di- σ bonding configuration would be associated with the EB structure rather than the OT structure. We also discuss the recent experimental data about the desorption of produced benzene and the formation of double di- σ bonding configuration.

DOI: 10.1103/PhysRevB.77.115329

PACS number(s): 68.43.Bc, 68.43.Mn, 68.43.Fg, 31.15.es

I. INTRODUCTION

The adsorption of organic molecules on semiconductor surfaces has attracted much attention because of its potential technological application for the formation of well-ordered organic-semiconductor interfaces as well as for the possibility of combining the wide range of functionality of organic molecules with the existing Si-based infrastructure.¹⁻³ Especially, for cyclic unsaturated hydrocarbons, such as cyclopentene⁴ and 1,5-cyclooctadiene,⁵ scanning tunneling microscopy (STM) experiments observed well-ordered monolayer films on the Si(001) surface. The reaction of such cyclic hydrocarbons with Si(001) has been explained by the so-called [2+2] cycloaddition mechanism where the interaction of the π bond of unsaturated hydrocarbons with the dangling bonds of a Si dimer produces two new Si—C σ bonds.^{3,4} The reaction path for the [2+2] product was theoretically predicted to have a small energy barrier through a π -complex precursor state which is composed of a three-membered ring with the two C atoms (bonded by a C=C double bond) and the down Si atom of the buckled dimer.⁶ In fact, this [2+2] cycloaddition reaction on Si(001) has been observed to be facile with a nearly unity sticking coefficient at room temperature.^{4,5,7}

For the fabrication of ordered monolayer film of cyclic unsaturated hydrocarbons, the adsorption of 1,4-cyclohexadiene on the Si(001) surface has also been experimentally⁸⁻¹⁴ and theoretically^{15,16} studied. Earlier photoelectron spectroscopy,⁸⁻¹⁰ vibrational spectroscopy,¹⁰⁻¹² and STM^{10,13,16} studies identified only one adsorption configuration as the single di- σ bonding configuration, i.e., the on-top (OT) structure [see Fig. 1(a)], where 1,4-cyclohexadiene adsorbs on top of a single Si dimer. On the theoretical side, first-principles density-functional theory (DFT) calculations¹⁵ showed that, although the double di- σ bonding structure [see Fig. 1(c)] where 1,4-cyclohexadiene adsorbs between two adjacent Si dimers is more thermody-

namically stable than the OT structure, the observation of the OT structure can be explained by the existence of a high activation barrier for the transition from the OT structure to the double di- σ bonding structure. Recently, using temperature-programmed desorption (TPD), low-energy electron diffraction, and high-resolution electron spectroscopy,

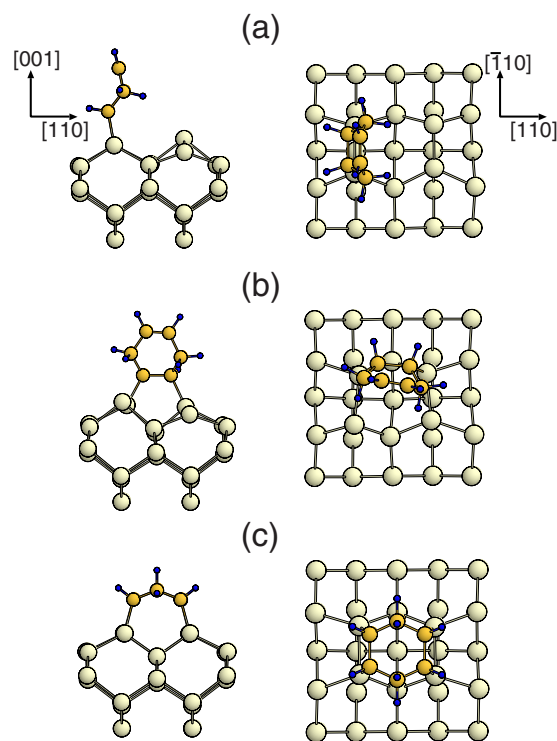


FIG. 1. (Color online) Side and top views of the optimized structure of adsorbed 1,4-cyclohexadiene on Si(001): (a) the OT structure, (b) the EB structure, and (c) the double di- σ bonding structure. The circles represent Si, C, and H atoms with decreasing size.

Kato *et al.*¹⁴ found that several adsorption configurations of 1,4-cyclohexadiene on Si(001) can be formed with a variation of substrate temperature: (i) Upon adsorption at 85 K, all adsorbed 1,4-cyclohexadiene molecules occupy the above-mentioned π -complex state. (ii) As substrate temperature increases to above 150 K, the π -complex state is chemically converted to a single di- σ bonding configuration (which was interpreted in terms of the OT structure). (iii) Upon further heating above 300 K, dehydrogenation of the single di- σ bonding configuration occurs, thereby producing an adsorbed benzene which immediately desorbs from the surface. (iv) Unlike the above three chemical processes, upon adsorption with low exposure at 300 K, 1,4-cyclohexadiene preferentially occupies the double di- σ bonding configuration. These recent experimental findings demand a more detailed theoretical study for the reaction paths which account for the dehydrogenation of single di- σ bonding configuration as well as the formation of double di- σ bonding configuration at 300 K.

In this paper, by using first-principles DFT calculations, we investigate not only the binding energy and structure of adsorbed 1,4-cyclohexadiene on Si(001) but also the reaction pathways for 1,4-cyclohexadiene adsorption. The initial reaction of 1,4-cyclohexadiene with Si(001) occurs via the π -complex state in which the electron-deficient down Si atom of the buckled dimer attracts the π bond of 1,4-cyclohexadiene. We consider the two different reaction pathways along which the π -complex state proceeds to the formation of the intradimer and interdimer products, i.e., the OT structure and the end-bridge (EB) structure [see Fig. 1(b)] across the ends of two adjacent Si dimers. Hereafter, the two reaction pathways are labeled as I and II, respectively. We find that along the reaction pathway I, dehydrogenation of the OT structure is kinetically difficult because of the existence of a high activation barrier of 1.34 eV, while along the reaction pathway II, dehydrogenation of the EB structure is kinetically facilitated at room temperature with a relatively lower activation barrier of 0.68 eV. Thus, we can say that the recently observed¹⁴ dehydrogenation process in the single di- σ bonding configuration would be associated with the EB structure rather than the OT structure. In addition, we study a concerted reaction of 1,4-cyclohexadiene on top of the two adjacent Si dimers within the symmetric-dimer model. As the two π bonds of 1,4-cyclohexadiene equally approach two adjacent symmetric dimers, we find a rapid increase of the adsorption energy, which indicates a facile formation of the double di- σ bonding configuration. By considering that the rate of the thermal flipping motion of buckled dimers increases with increasing temperature, this result may provide an explanation for a recent experimental data¹⁴ that the double di- σ bonding configuration is preferentially occupied upon adsorption at room temperature.

II. CALCULATIONAL METHOD

The total-energy and force calculations were performed by using first-principles DFT within the generalized-gradient approximation.¹⁷ We used the exchange-correlation functional of Perdew *et al.*¹⁸ for the the generalized-gradient ap-

TABLE I. Calculated adsorption energies (in eV) per molecule for various adsorption configurations such as the precursor (*P*), transition (*T*), dissociative (*D*), OT, EB, and double di- σ bonding structures. Each structure is displayed in Figs. 2 and 3.

		E_{ads}
Path I	P_{OT}	0.35
	$T_{\text{OT-1}}$	0.09
	OT	1.33
	$T_{\text{OT-2}}$	-0.01
	$D_{\text{OT-1}}$	0.92
	$T_{\text{OT-3}}$	0.95
	$D_{\text{OT-2}}$	2.20
	Path II	P_{EB}
$T_{\text{EB-1}}$		0.07
EB		1.09
$T_{\text{EB-2}}$		0.41
$D_{\text{EB-1}}$		1.04
$T_{\text{EB-3}}$		1.07
$D_{\text{EB-2}}$		2.13
Double di- σ		2.50

proximation. The norm-conserving pseudopotentials of Si and H atoms were constructed by the scheme of Troullier and Martins¹⁹ in the separable form of Kleinman and Bylander.²⁰ For carbon whose 2*s* and 2*p* valence orbitals are strongly localized, we used the Vanderbilt ultrasoft pseudopotentials.²¹ The surface was modeled by a periodic slab geometry. Each slab contains six Si atomic layers, and the bottom Si layer was passivated by two H atoms per Si atom. The thickness of the vacuum region between these slabs is about 13 Å, and 1,4-cyclohexadiene molecules are adsorbed on the unpassivated side of the slab. To make the interaction between adsorbed molecules sufficiently weak, we employed a 2×4 unit cell that involved four dimers along the dimer row. A plane-wave basis set was used with 25 Ry cutoff, and a **k** space integration was done with meshes of two **k** points in the 2×4 surface Brillouin zone. All the atoms except the bottom two Si layer allowed us to relax along the calculated Hellmann–Feynman forces until all the residual forces components were less than 1 mRy/bohr. Our calculation scheme has been successfully applied to the adsorption and reaction of various cyclic unsaturated hydrocarbons on Si(001).^{15,22,23}

III. RESULTS

We first determined the atomic structure of adsorbed 1,4-cyclohexadiene on Si(001) within the OT, EB, and double di- σ bonding structures. Each optimized structure is displayed in Fig. 1. The calculated adsorption energies (E_{ads}) for these structures are given in Table I. We find that the OT, EB, and double di- σ bonding structures have $E_{\text{ads}}=1.33$, 1.09, and 2.50 eV, respectively. In the EB structure, we note that the formation of two Si—C σ bonds between two neighboring

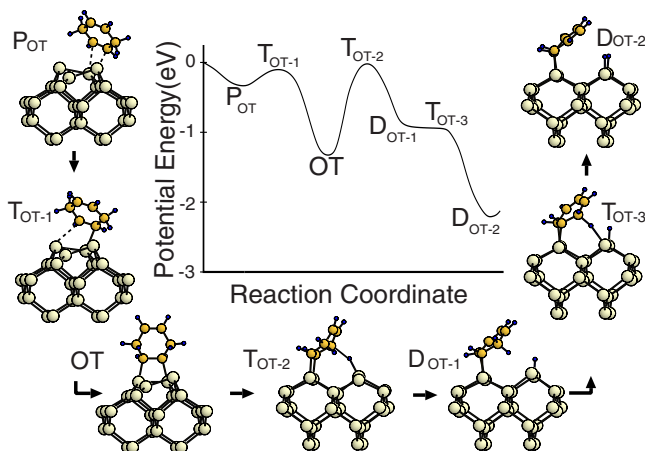


FIG. 2. (Color online) Calculated energy profile for the reaction pathway I, forming the OT structure as well as its dissociative states. The atomic geometries of the precursor (P), transition (T), and dissociative (D) states are also given. The reaction coordinate between P_{OT} and OT is the distance d_{C-Si} (represented by the dashed line in T_{OT-1}) between the C atom and its bonded Si atom (in the OT structure), while that after the formation of OT is the bond length d_{C-H} between the dissociating H atom and its bonded C atom.

Si dimers breaks π bonds on both of the two dimers, and thus render the remaining single Si dangling bonds chemically very reactive. Here, we find two different dimer-bond lengths [$d_{Si-Si}=2.45$ and 2.40 Å for the left- and right-side dimers in Fig. 1(b)] for the reacted Si dimers. These values in the EB structure are longer than $d_{Si-Si}=2.35$, 2.36 , and 2.35 Å of the clean Si(001) surface, the OT structure, and the double di- σ bonding structure, respectively. The electronic states of highly reactive single dangling bonds in the EB structure lie close to the Fermi level compared to those of dangling bonds in the clean buckled dimer, therefore contributing to the relatively less energetic stability of the EB structure compared to the OT structure. We also note that the OT and EB structures which belong to the same di- σ bonding configuration are formed through the intradimer and interdimer reactions of 1,4-cyclohexadiene, respectively. Recently, there have been a number of experimental^{24,25} and theoretical²⁶⁻²⁸ reports on the intradimer and interdimer reactions of unsaturated hydrocarbons on Si(001). However, all previous experimental⁸⁻¹⁴ and theoretical^{15,16} studies have not considered the interdimer reaction which results in the formation of the EB structure.

It is well known that the chemisorption of unsaturated hydrocarbons on Si(001) takes place via a weakly bound π -complex precursor which is composed of a three-membered ring with the two C atoms and the down Si atom of the buckled dimer.^{22,29,30} This precursor state can be easily produced because of the energetically favored hybridization between the π bonding state of unsaturated hydrocarbons and the empty dangling-bond state of the down Si atom. For adsorbed 1,4-cyclohexadiene, such a precursor state (designated as P_{OT}) is found to have an adsorption energy $E_{ads}=0.35$ eV. As shown in Fig. 2, the reacted C=C bond in P_{OT} lies in the same ($\bar{1}10$) plane as the Si dimer. We also find

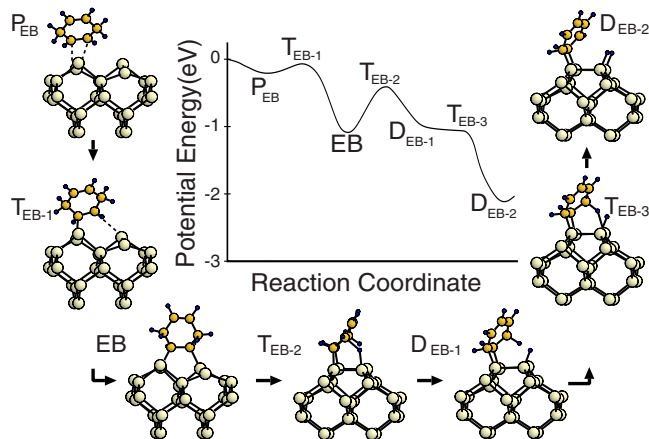


FIG. 3. (Color online) Calculated energy profile for the reaction pathway II, forming the EB structure as well as its dissociative states. The atomic geometries of the precursor (P), transition (T), and dissociative (D) states are also given. The reaction coordinate between P_{EB} and EB is the distance d_{C-Si} (represented by the dashed line in T_{EB-1}) between the C atom and its bonded Si atom (in the EB structure), while that after the formation of EB is the bond length d_{C-H} between the dissociating H atom and its bonded C atom.

an additional precursor state (designated as P_{EB} , see Fig. 3) with $E_{ads}=0.22$ eV, where the reacted C=C bond is in the (110) plane perpendicular to the Si dimer. Since the P_{OT} state is more stable than the P_{EB} state by $\Delta E_{ads}=0.13$ eV, we expect that at extremely low temperature adsorbed 1,4-cyclohexadiene might mostly occupy the P_{OT} state. This is consistent with a recent experimental data¹⁴ that upon adsorption at 85 K, all adsorbed 1,4-cyclohexadiene molecules were trapped at the π -complex state. We note that the barrier for the rotation of the π -complex state (from P_{OT} to P_{EB}) amounts to ~ 0.14 eV. Therefore, as temperature increases, the rotation of the π -complex state is likely to be easily thermal activated.

Next, we study the reaction pathway I (II) from the P_{OT} (P_{EB}) state to the OT (EB) structure. In order to find the minimum energy pathway, we optimize the structure by using the gradient projection method³¹ where only the distance d_{C-Si} (represented by the dashed line in the T_{OT-1} and T_{EB-1} states, see Figs. 2 and 3) between the C atom and its bonded Si atom (in the OT and EB structures) is constrained. Therefore, we obtain the energy profiles for the reaction pathways I and II as a function of decreasing the distance d_{C-Si} . Here, Hellmann-Feynman forces are used for the relaxation of all the atomic positions as well as the C—Si bond angles for each fixed value of d_{C-Si} . The calculated energy profiles and the atomic geometries of the transition states (T_{OT-1} and T_{EB-1}) along the reaction pathways I and II are displayed in Figs. 2 and 3, respectively. We find that the T_{OT-1} (T_{EB-1}) state has $E_{ads}=0.09$ (0.07) eV, which is 0.26 (0.15) eV smaller than that of the P_{OT} (P_{EB}) state, thereby yielding an energy barrier (E_b) of 0.26 (0.15) eV from the P_{OT} (P_{EB}) state to the OT (EB) structure. By using an Arrhenius-type activation process with a typical vibration frequency (10^{13} Hz) for the preexponential factor, we estimate that at

150 K, the reaction rate from the P_{OT} (P_{EB}) state to the OT (EB) structure is $\sim 1.9 \times 10^4$ (9.3×10^7) s^{-1} , indicating that formations of the OT and EB structures are kinetically facilitated. This is consistent with the recent experimental data¹⁴ that as substrate temperature increases to above 150 K, the π -complex state is converted to a di- σ bonding configuration. We note that the observed di- σ bonding configuration was interpreted in terms of the OT structure.¹⁴ However, our analysis for the reaction rates shows that at 150 K, the EB structure is likely to be more occupied as compared to the OT structure.

According to the recent experimental data,¹⁴ the dehydrogenation of di- σ bonding configuration occurs upon heating above 300 K after exposure at low temperatures. To examine this dehydrogenation process, we calculated the energy profile for the cleavage of the C—H bond by optimizing the structure with increasing the bond length d_{C-H} . Figure 2 shows the calculated energy profile and the atomic geometries of the transition (designated as T_{OT-2} and T_{OT-3}) and dissociative (designated as D_{OT-1} and D_{OT-2}) states along the reaction pathway I. Note that there are two H-dissociation steps. The first C—H bond cleavage occurs via the transfer of the H atom to the electron-abundant up Si atom of the neighboring dimer. For the first C—H bond cleavage, we obtain an energy barrier $E_b = 1.34$ eV from the OT structure to the D_{OT-1} state. However, after the first H dissociation, the energy profile monotonically slopes between the D_{OT-1} and T_{OT-3} states by 0.03 eV, indicating that the second C—H bond cleavage takes place without any barrier. Here, the T_{OT-3} state represents a quasitransition state just before the rapid energy descent along the reaction pathway. Since the D_{OT-1} (T_{OT-3}) state is not at an energy minimum (maximum), their exact positions on the reaction pathway are not uniquely defined. We have to note that our previous¹⁵ DFT calculations obtained an energy barrier of 0.95 eV for the transition from the OT to the double di- σ bonding structure, which is lower than the present dehydrogenation barrier of 1.34 eV from the OT structure. Thus, we can say that the OT structure will be converted to the double di- σ bonding structure before its dehydrogenation. Compared to the reaction pathway I, Fig. 3 shows the calculated energy profile and the atomic geometries of the transition (designated as T_{EB-2} and T_{EB-3}) and dissociative (designated as D_{EB-1} and D_{EB-2}) states along the reaction pathway II. We obtain $E_b = 0.68$ eV for the first C—H bond cleavage (from the EB structure to the D_{EB-1} state) and no barrier for the second C—H bond cleavage. On the basis of our calculated energy barriers for the H-dissociation processes, Arrhenius-type analysis estimates the reaction rate for the dehydrogenation of the EB structure as ~ 40 s^{-1} at 300 K. Thus, it is likely that the observed¹⁴ dehydrogenation of single di- σ bonding configuration would be associated with the EB structure rather than the OT structure. The relatively lower energy barrier for the dehydrogenation of the EB structure is due to the presence of highly reactive single dangling bonds which can more easily abstract H atoms from an end-bridge 1,4-cyclohexadiene. Figure 4 shows the schematic diagram of frontier orbital interactions in the dehydrogenation. In the EB structure, $\pi_{Si-dimer}$ and $\pi_{Si-dimer}^*$ correspond to the electronic states of highly reactive single dangling bonds that lie close to the Fermi level

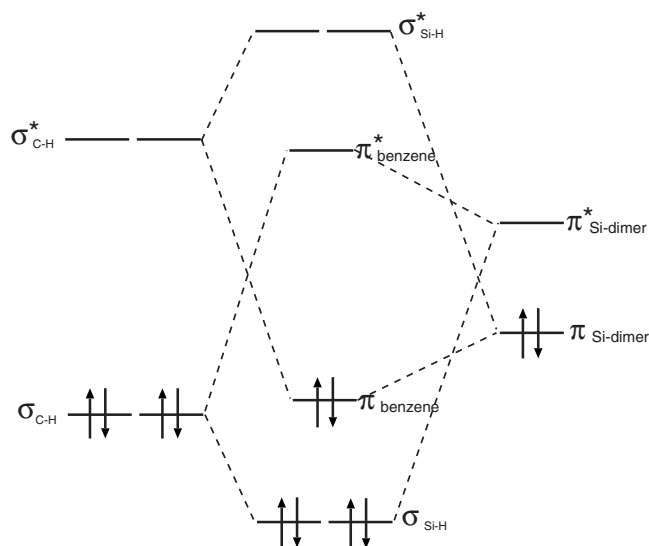


FIG. 4. Schematic diagram of frontier orbital interactions in the dehydrogenation.

compared to those in the OT structure. Thus, the energy difference between $\pi_{Si-dimer}$ and $\pi_{Si-dimer}^*$ in the EB structure is reduced, thereby giving rise to an enhanced hybridization with σ_{C-H} and σ_{C-H}^* states.

From the TPD data, Kato *et al.*¹⁴ inferred that after dehydrogenation, the produced benzene immediately desorbs from the surface. To support this inference, we calculate the desorption energy of the produced benzene, which is defined as the difference in the total energy of the D_{EB-2} state from its separated limit with a free benzene molecule and the Si substrate containing two attached H atoms. We find that such a desorption energy is only 0.44 eV. This value indicates that the desorption of the produced benzene will be facilitated at temperatures above 300 K, which is in accordance with the TPD data.¹⁴

To simulate adsorption at room temperature, we consider a concerted reaction of 1,4-cyclohexadiene on Si(001) within the symmetric-dimer model. Note that at room temperature STM experiments have shown symmetric dimer images which are ascribed to thermal activated flipping motion of bucked dimers.³²⁻³⁴ As the two π bonds of 1,4-cyclohexadiene equally approach two adjacent symmetric dimers, we find a rapid increase of the adsorption energy, indicating an attractive interaction between the π bonds of 1,4-cyclohexadiene and the dangling bonds of symmetric dimers. Thus, we can say that this concerted reaction leads to a facile formation of the double di- σ bonding structure. This may provide an explanation for a recent experimental observation¹⁴ that upon adsorption at room temperature, the double di- σ bonding configuration is preferentially formed.

STM has proved to be a powerful tool for a direct view of adsorbed organic molecules on Si(001). Yoshinobu and co-workers^{10,13,16} performed STM studies for 1,4-cyclohexadiene adsorbed on Si(001) at room temperature. In their STM images, Yoshinobu and co-workers^{10,13,16} identified two different adsorption configurations as the differently tilted single di- σ bonding configurations, but later¹⁴ such as-

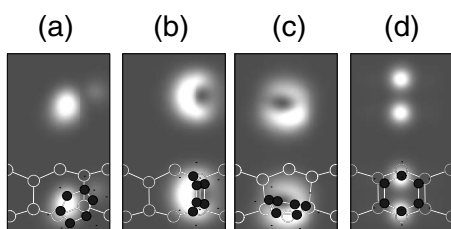


FIG. 5. Simulated filled-state STM images of adsorbed 1,4-cyclohexadiene on Si(001): (a) the π -complex precursor state, (b) the OT structure, (c) the EB structure, and (d) the double di- σ bonding structure. The filled-state images were obtained by integrating the charge from occupied states within 3 eV of the highest occupied state. The images were taken at 2.2 Å above the outermost C atom. The small dark and large open circles represent the positions of the C and the first and second Si layer atoms, respectively.

segment was modified to be in terms of the single and double di- σ configurations. To our knowledge, there is no STM study for 1,4-cyclohexadiene adsorbed on Si(001) at low temperatures. We anticipate that future STM studies with a variation of substrate temperature will observe the presence of the π -complex state and its conversion to the single di- σ bonding configurations such as the OT and EB structures. Thus, it is helpful to compare the simulated STM images for several adsorption configurations such as the π -complex, OT, EB, and double di- σ bonding structures. As shown in Fig. 5, we find disparate features in the simulated filled-state STM images among those adsorption structures. In our previous DFT study,¹⁵ we have already pointed out a conspicuous difference in the features of STM images between the OT and double di- σ bonding structures. The OT structure containing the π orbital of the unreacted C=C bond produces a single bright spot in one side of the C=C bond, while the double di- σ bonding structure produces the two

bright spots in the center region between two Si dimers. It is expected that the images of the OT and EB structures might be similar to each other except the different locations of their single bright spots. However, it is noticeable that the image of the OT structure is almost symmetric with respect to a plane bisecting the unreacted C=C bond, but that of the EB structure is asymmetric due to the different heights of the two C atoms bonded by the unreacted C=C bond. We also note that the image of the EB structure shows brightness in both sides of the unreacted C=C bond, contrasting with that of the OT structure. In the π -complex state, the image shows a single bright spot on top of adsorbed 1,4-cyclohexadiene.

IV. SUMMARY

We have performed first-principles density-functional calculations for the adsorption of 1,4-cyclohexadiene on Si(001). Our calculated energy profiles for the reaction pathways showed that the π -complex precursor state is easily converted to the single di- σ bonding configurations such as the OT and EB structures. Especially, we found that dehydrogenation of the EB structure is kinetically feasible at room temperature with its relatively lower activation barrier, while that of the OT structure is not. Thus, the recently observed¹⁴ dehydrogenation of the single di- σ bonding configuration can be associated with the EB structure rather than the OT structure. We also suggested that the thermal activated flipping motion of bucked dimers may play an important role in the formation of the double di- σ bonding configuration.

ACKNOWLEDGMENT

This work was supported by the MOST/KO SEF through the Quantum Photonic Science Research Center.

*Correspondence author; chojh@hanyang.ac.kr

¹R. A. Wolkow, *Annu. Rev. Phys. Chem.* **50**, 413 (1999).

²S. F. Bent, *Surf. Sci.* **500**, 879 (2002).

³R. J. Hamers, S. K. Coulter, M. D. Ellison, J. S. Hovis, D. F. Padowitz, M. P. Schwartz, C. M. Greenlief, and J. N. Russell, Jr., *Acc. Chem. Res.* **33**, 617 (2000).

⁴R. J. Hamers, J. S. Hovis, S. Lee, H. Liu, and J. Shan, *J. Phys. Chem.* **101**, 1489 (1997); J. S. Hovis, H. Liu, and R. J. Hamers, *Surf. Sci.* **402**, 1 (1998).

⁵J. S. Hovis and R. J. Hamers, *J. Phys. Chem.* **101**, 9581 (1997).

⁶J.-H. Cho and L. Kleinman, *Phys. Rev. B* **67**, 115314 (2003).

⁷F. Jolly, F. Bournel, F. Rochet, G. Dufour, F. Sirrotti, and A. Taleb, *Phys. Rev. B* **60**, 2930 (1999).

⁸K. Hamaguchi, S. Machida, K. Mukai, Y. Yamashita, and J. Yoshinobu, *Phys. Rev. B* **62**, 7576 (2000).

⁹Y. Yamashita, K. Hamaguchi, S. Machida, K. Mukai, J. Yoshinobu, S. Tanaka, and M. Kamada, *Appl. Surf. Sci.* **169-170**, 172 (2001).

¹⁰K. Hamaguchi, S. Machida, M. Nagao, F. Yasui, K. Mukai, Y. Yamashita, J. Yoshinobu, H. Kato, H. Okuyama, M. Kawai, T.

Sato, and M. Iwatsyki, *J. Phys. Chem. B* **105**, 3718 (2001).

¹¹M. J. Kong, A. V. Teplyakov, J. Jagmohan, J. G. Lyubovitsky, C. Mui, and S. F. Bent, *J. Phys. Chem. B* **104**, 3000 (2000).

¹²M. Wakatsuchi, H. S. Kato, H. Fujisawa, and M. Kawai, *J. Electron Spectrosc. Relat. Phenom.* **137-140**, 217 (2004).

¹³K. Hamaguchi, K. Mukai, Y. Yamashita, J. Yoshinobu, T. Sato, and M. Iwatsyki, *Surf. Sci.* **531**, 199 (2003).

¹⁴H. S. Kato, M. Wakatsuchi, M. Kawai, and J. Yoshinobu, *J. Phys. Chem. C* **111**, 2557 (2007).

¹⁵J.-H. Cho and D.-H. Oh, K. S. Kim, and L. Kleinman, *J. Chem. Phys.* **116**, 3800 (2002).

¹⁶K. Akagi, S. Tsuneyuki, Y. Yamashita, K. Hamaguchi, and J. Yoshinobu, *Appl. Surf. Sci.* **234**, 162 (2004).

¹⁷P. Hohenberg and W. Kohn, *Phys. Rev.* **136**, B864 (1964); W. Kohn and L. J. Sham, *Phys. Rev.* **140**, A1133 (1965).

¹⁸J. P. Perdew, K. Burke, and M. Ernzerhof, *Phys. Rev. Lett.* **77**, 3865 (1996).

¹⁹N. Troullier, and J. L. Martins, *Phys. Rev. B* **43**, 1993 (1991).

²⁰L. Kleinman and D. M. Bylander, *Phys. Rev. Lett.* **48**, 1425 (1982).

- ²¹D. Vanderbilt, Phys. Rev. B **41**, 7892 (1990); K. Laasonen, A. Pasquarello, R. Car, C. Lee, and D. Vanderbilt, *ibid.* **47**, 10142 (1993).
- ²²J.-H. Cho and L. Kleinman, Phys. Rev. B **64**, 235420 (2001).
- ²³J.-H. Cho, D. H. Oh, and L. Kleinman, Phys. Rev. B **64**, 241306(R) (2001).
- ²⁴S. Mezhenny, I. Lyubnitsky, W. J. Choyke, R. A. Wolkow, and J. T. Yates, Jr., Chem. Phys. Lett. **344**, 7 (2001).
- ²⁵W. Kim, H. Kim, G. Lee, Y. K. Hong, K. Lee, C. Hwang, D. H. Kim, and J. Y. Koo, Phys. Rev. B **64**, 193313 (2001).
- ²⁶X. Lu and M. Zhu, Chem. Phys. Lett. **393**, 124 (2004).
- ²⁷J.-H. Cho and L. Kleinman, Phys. Rev. B **69**, 075303 (2004).
- ²⁸P. Minary and M. E. Tuckerman, J. Am. Chem. Soc. **127**, 1110 (2005).
- ²⁹Q. Liu and R. J. Hoffmann, J. Am. Chem. Soc. **117**, 4082 (1995).
- ³⁰H. Liu and R. Hamers, J. Am. Chem. Soc. **119**, 7593 (1997).
- ³¹D. A. Wismer and R. Chatter, *Introduction to Nonlinear Optimization* (North-Holland, Amsterdam, 1978), pp. 174–178.
- ³²R. M. Tromp, R. J. Hamers, and J. E. Demuth, Phys. Rev. Lett. **55**, 1303 (1985); R. J. Hamers, R. M. Tromp, and J. E. Demuth, Phys. Rev. B **34**, 5343 (1986).
- ³³J. Dabrowski and M. Scheffler, Appl. Surf. Sci. **56**, 15 (1992).
- ³⁴Y. Fukaya and Y. Shigeta, Phys. Rev. Lett. **91**, 126103 (2003).